Melting in three-dimensional and two-dimensional Yukawa systems

O. S. Vaulina and X. G. Koss*

Joint Institute for High Temperatures RAS, 125412, Izhorskaya St. 13 Bd. 2, Moscow, Russia
and Moscow Institute of Physics and Technology, 141700, Institutskiy Pereulok 9, Dolgoprudny, Russia

(Received 3 June 2015; revised manuscript received 14 August 2015; published 28 October 2015)

Solid-liquid phase transitions in three-dimensional (3D) and two-dimensional (2D) Yukawa systems were studied numerically and analytically, including the melting of the fcc and bcc 3D lattices, and of a hexagonal primitive (hp) 2D lattice. An approach is proposed for the determination of the melting lines in these systems. The suggested approach takes into account the nonlinearity (anharmonicity) of pair interaction forces and allows one to correctly predict the conditions of melting for 3D and 2D crystal systems. The obtained results are compared with the existing theoretical and numerical data.

DOI: 10.1103/PhysRevE.92.042155 PACS number(s): 64.60.Ej, 64.70.dj, 07.05.Tp

I. INTRODUCTION

The study of phase transitions is of significant interest from a fundamental point of view and, at present, it is a subject of intensive theoretical and experimental research in various areas of physics [1–7]. The calculation of phase diagrams for strongly coupled two-dimensional (2D) and three-dimensional (3D) systems is usually performed with the help of numerical techniques (Monte Carlo or molecular dynamics methods). As the criteria of a phase transition, various physical relationships are used, e.g., the minimum of Helmholtz free energy or of internal energy density, the abrupt changes in the diffusion and/or viscosity constants, the changes of spatial and/or thermal dependencies of the pair and orientational correlation functions, etc. [8–46]. The obtained numerical data are commonly presented in the form of some parametrical functions (the various polynomial fittings, or the half-empirical approximations), which depend on the type and parameters of pair potentials, as well as on the segment of the analyzed melting curve [7–22,42–46]. In any case, this approach does not show how the conditions of melting change with the variations of interparticle interaction potential. Besides, the majority of existing numerical data both for 2D and 3D systems concern the pure dispersive (frictionless) case, when the friction coefficient of particles $\nu_{fr} = 0$ [8–13,17–21,34–46].

Here we present the results of numerical and theoretical studies of phase transitions between the liquid and solid phases for the dissipative systems ($\nu_{fr} \neq 0$) of particles interacting with of Yukawa-type potentials with interaction energy as follows:

$$\phi(r) = (eZ)^2 \exp(-r/\lambda)/r, \tag{1}$$

where eZ is the particle charge, r is the distance between particles, and λ is the screening length (hereafter we use the cgs electrostatic units). This type of potential is commonly applied within the framework of physical kinetics for the description of the interaction in various systems, e.g., in the physics and chemistry of polymers, in medicine, biology, and complex plasma [1–7]. Note that the model of screened Yukawa potential (1) has been successfully used for the analysis of results of various experiments [1–4,10,14], for example, for the description of the phase transition in samples of polystyrene spheres in the water [10], and also for the study of dynamics of dust particles in laboratory plasma [4–6,26,47]. In both of the last cases, the dissipation caused by the collisions of the charged grains with the neutral particles of the surrounding medium ($\nu_{fr} \neq 0$) may substantially affect the transport characteristics of the ordered structures.

For the wide range of 3D systems with various repulsive isotropic potentials $\phi \equiv \phi(r)$, where $2\pi > |\phi^{(2)} r_p/\phi^{(1)}|$, the melting of the bcc crystal lattice is well described by the criterion suggested in [14–16,22,23,48]

$$\Gamma^* \equiv \Gamma^*_M \cong 104.5 \pm 5. \tag{2}$$

Here Γ^* is the effective coupling parameter defined as

$$\Gamma^* = r_p^2 \phi^{(2)}/(2T), \tag{3}$$

where T is the temperature of particles (in energy units); $\phi^{(1)}$, $\phi^{(2)}$ are the first and second derivatives of energy $\phi(r)$ at the point of $r = r_p$, respectively; $r_p = n^{-1/m}$ is the mean interparticle distance, where n is the concentration of particles; and $m = 2,3$ is the number of dimensions of systems. For the Yukawa systems, $\Gamma^* = \Gamma(1 + \kappa + \kappa^2/2)\exp(-\kappa)$, where $\Gamma = (eZ)^2/(r_p T)$ is the Coulomb coupling parameter, and $\kappa \equiv r_p/\lambda$ is the screening parameter.

We should note that, according to recent studies, the mentioned criterion (2) also describes the phase transition between the liquid and bcc phases in the systems with inverse power-law potentials [48] and the phase transition between the liquid and fcc phases in Lennard-Jones systems with certain parameters of the interaction potential [49]. Nevertheless, the differences in the position of the melting curve of fcc lattice from the criterion given by (2) become essential in the Yukawa system with the increase of κ [14–16,48].

As for 2D Yukawa systems, the data on conditions of their melting are significantly different. So, in a number of works it is observed that a two-stage process of melting via the intermediate, so-called "hexatic" phase [23–29,31,35,37] in accordance with the Kosterlitz-Thouless-Halperin-Nelson-Young (KTHNY) theory [50–52] takes place; in other works the formation of any intermediate phase in the solid-liquid transitions was found [32–34,36,38]. At that, the values of coupling parameter Γ^* at the melting lines of a "perfect" 2D crystal with the hp lattice can vary in a wide range:

*Xeniya.Koss@gmail.com

from ∼60−80 [31,36–41] (by use of the analysis of the orientational correlation function or the global orientational order parameter) to ∼100 [23–29,32–35] (by the results of the analysis of temperature dependence of the internal energy of system $U(T)$, the Lindemann parameter, the diffusion constant of particles, etc.).

The numerical experiments in dissipative 2D Yukawa systems with $\nu_{fr} \neq 0$ show that their physical characteristics (e.g., the pair and orientational correlation functions, the pressure and the internal energy density, the heat capacity, the diffusion and viscosity constants, etc.) have two singularities [23–29]. The first corresponds to the "liquid-hexatic" phase transition and is observed when the effective coupling parameter $\Gamma^* \approx 65 \pm 3$; the second singular point is due to the transition from the hexatic phase to the "perfect" crystal, where the diffusion coefficient of the particles $D \to 0$, which corresponds to

$$\Gamma^* \equiv \Gamma^*_M \cong 102.5 \pm 4, \tag{4}$$

very close to criterion (2), suggested for 3D systems. Note that Clark *et al.* [35] obtained similar values of Γ^* on the phase boundaries for the Coulomb systems ($\kappa = 0$) in the frictionless case of $\nu_{fr} = 0$ by the analysis of temperature dependence of the internal energy of system $U(T)$ using the quantum Monte Carlo method in the classical limit of the problem. Furthermore, melting conditions similar to Eq. (4) have also been obtained for frictionless 2D Yukawa systems ($\kappa = 2,3,4$) as a result of the analysis of the Lindemann parameter [34]. Note that the criterion (4) well describes the melting conditions for quasi-2D systems (i.e., the systems with additional degree of freedom in the direction orthogonal to a two-dimensional monolayer), both for the numerical simulation [23,24] and for the laboratory experiments [26,30].

In this work we propose an analytical approximation for the locating of melting lines for the fcc, bcc, and hexagonal primitive (hp) lattices in the Yukawa systems. Unlike existing approximations [7–22,42–46], the proposed approach does not lean upon the empirical fitting of numerical data by arbitrary polynomial functions and/or on the semiempirical models (which are based on the simple harmonic or quasiharmonic approximations) and can be used for the analysis of the melting conditions with the changes of interparticle interactions in a wide range of screening parameters.

Here we present two alternative methods to determine the melting point of 2D and 3D Yukawa systems. The first of them, based on molecular dynamics simulations, is described in Sec. II (which includes the parameters of numerical problems, the results of simulations, and their comparison with the existing theoretical and numerical data). The second method, based on a theoretical analysis of correlation quantities, is described in Sec. III (which includes analytical approaches for equilibrium melting curves and for the thermal fluctuations of the electric field, as well as a comparison of the obtained theoretical relationships with the various numerical data).

II. NUMERICAL SIMULATIONS

The numerical simulations were carried out by the Langevin molecular dynamics method (under the periodic boundary conditions) based on the solution of the system of N_p ordinary differential equations, N_p being the number of the independent particles in a computational cell. The stochastic character of motion of the particles with the given kinetic temperature T was determined by the Langevin force F_{ran}. [The latter takes into account processes leading to the established equilibrium (stationary) kinetic temperature T of particles that characterizes kinetic energy of their random (thermal) motion according to the fluctuation-dissipation theorem.] The simulation technique is detailed in [4,5].

In the 3D case, the periodical boundary conditions were used for all three directions x, y, and z. The calculations were carried out for the Yukawa systems with the values of screening parameter $\kappa \equiv r_p/\lambda$ from 2 to 12. The number of independent particles N_p in the central calculated cell (a cubic box) was varied from ∼250 to ∼2500; accordingly, the cutoff distance r_{cut} of the potential was varied from $4r_p$ to $10r_p$ (here $r_p = (N_p/V_c)^{1/3}$, where V_c is the volume of simulated cell). The majority of data were obtained for $N_p = 500$ for the fcc lattice and $N_p = 686$ for the bcc lattice with $r_{cut} = 7r_p$, because the further increase of the number of particles did not lead to a substantial change of the numerical results.

In the 2D case, the simulations were carried out for a monolayer of grains with periodical boundary conditions in the directions x and y for the Yukawa systems with the screening parameters $\kappa \equiv r_p/\lambda$ from 2 to 8 [where $r_p = (N_p/S)^{1/2}$, and S is the area of the computational cell]. The number of independent particles N_p in the central computational cell (a box with aspect ratio of $2 : \sqrt{3}$) was varied from 256 to 4096. Depending on the number of particles, the cutoff length of potential r_{cut} changed from $5r_p$ to $25r_p$. The majority of data were obtained for $N_p = 1024$ independent particles and $r_{cut} = 12r_p$.

For the analysis of the melting process the equations of motion were solved for various values of effective parameters: the coupling parameter Γ^* and the scaling parameter $\xi = \omega^*/\nu_{fr}$, where $\omega^* = \{\phi^{(2)}/(2M)\}^{1/2} \equiv \{(eZ)^2(1+\kappa+\kappa^2/2)\exp(-\kappa)/(r_p^3 M)\}^{1/2}$, and M is the mass of the particle.

The value of the scaling parameter was varied from $\xi \approx 0.4$ to $\xi \approx 4$, which is typical, for example, for grains in weakly ionized plasma, where the friction of particles is determined by their collisions with the neutrals of surrounding gas [4–6]. The value of the effective coupling parameter Γ^* was varied in the range from 90 to 150 (with the step $\Delta\Gamma^* \approx 2$ near the phase transition point).

Under initial conditions (for $\Gamma^* = 90$) the simulated systems were liquid structures with the diffusion constant $D \geqslant 0$. As the criterion of the phase transition, the jump of the diffusion coefficient D of the particles was used. A similar method (as the criterion of the crystallization of the system) was used in [14–16]. In other words, the parameters of the system were fixed in the moment when $D \to 0$, and the magnitude of mean-square displacement of particles from their equilibrium position in the nodes of the crystal lattice $\langle \delta r^2 \rangle \to$ const. (For the solid phase the values of $D = 0$, $\langle \delta r^2 \rangle =$ const.) Hereafter the angular brackets denote the ensemble (N) and time (t) averaging (the average is for all time intervals t).

We have estimated the following quantities near this point: the Lindemann parameter $\delta_L = \langle \delta r^2 \rangle^{1/2}/r_p$, the coupling parameter Γ^*, and the magnitude of the thermal fluctuations

TABLE I. The Lindemann parameter δ_L, the coefficients $C_F = \langle \delta F^2 \rangle / (r_p^2 M^2 \omega^{*4})$, and the coupling parameter $\Gamma^* = \Gamma_M^*$ on the melting lines of different lattices.

Lattice	δ_L ($\pm 2\%$)	C_F ($\pm 3\%$)	Γ_M^* ($\pm 3\%$)
bcc ($\kappa \sim 0 \div 7$)	0.136	0.38	$100 \div 110$
fcc ($\kappa \sim 7 \div 12$)	0.129	0.41	$110 \div 150$
hp ($\kappa \sim 0 \div 8$)	0.107	0.19	$98 \div 106$

of pair forces $\langle \delta F^2 \rangle = (eZ)^2 \langle \delta E^2 \rangle$ (and the fluctuations of the electric field δE, correspondingly), acting on the separate particle of the simulated equilibrium system.

It was obtained that $\delta_L \cong 0.136 \pm 2\%$ for the bcc lattice, $\delta_L \cong 0.129 \pm 2\%$ for the fcc lattice, and $\delta_L \cong 0.107 \pm 2\%$ for the hp lattice, respectively. Additionally, we have found that the magnitude of the fluctuations of the pair forces $\langle \delta F^2 \rangle$ in the simulated systems was proportional to ω^{*4}, namely, $\langle \delta F^2 \rangle \cong C_F r_p^2 M^2 \omega^{*4}$, where $C_F \cong 0.38 \pm 0.012$ for the bcc lattice, $C_F \cong 0.41 \pm 0.012$ for the fcc structure, and $C_F \cong 0.19 \pm 0.006$ for the hp lattice. (Note that the results of the simulation practically did not depend on the values of ξ; the difference between the measured quantity and its average value did not exceed the numerical error of $\pm 2\%$–3%.) The obtained numerical data are presented in Table I and shown in Figs. 1–3. So, the values of the coupling parameters $\Gamma^*(\kappa) = \Gamma(1 + \kappa + \kappa^2/2)\exp(-\kappa)$ on the melting lines of the 3D and 2D Yukawa systems are shown in Figs. 1 and 2, respectively, together with numerical data of various works [8–11,31–35]; the coefficients $C_F = \langle \delta F^2 \rangle / (r_p^2 M^2 \omega^{*4})$ for the 3D systems are presented in Fig. 3.

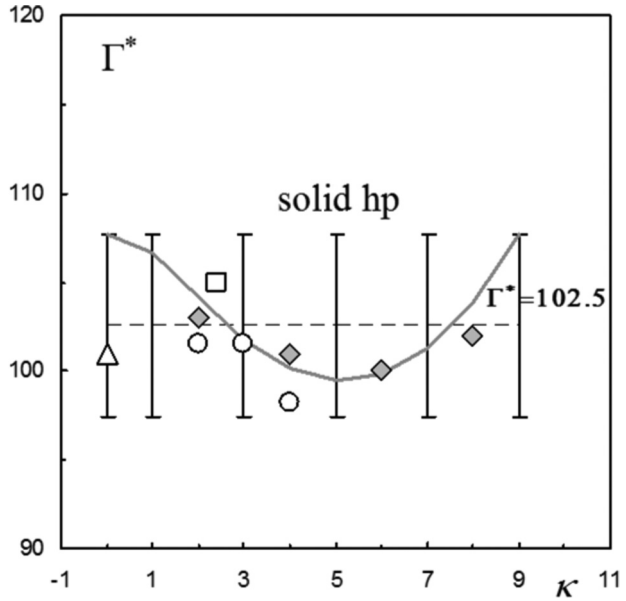

FIG. 2. Melting curves $\Gamma^*(\kappa)$ for the 2D Yukawa systems. The symbols correspond to the numerical simulation results: (■) the results presented in this paper; (□) Ref. [31]; (○) Refs. [32,34]; (△) Ref. [35]. The solid gray line denotes the analytical curve (12). The symbols (○) (△) correspond to frictionless systems; the symbols (□)(◆) correspond to dissipative structures.

Note that the type of crystal lattice in the 3D numerical simulation has changed from bcc to fcc for $\kappa > 7$, which agrees well with the numerical data [8–11] calculated for frictionless systems ($\xi \to \infty$; $\nu_{fr} \to 0$) (see Fig. 1). It is easy to see that

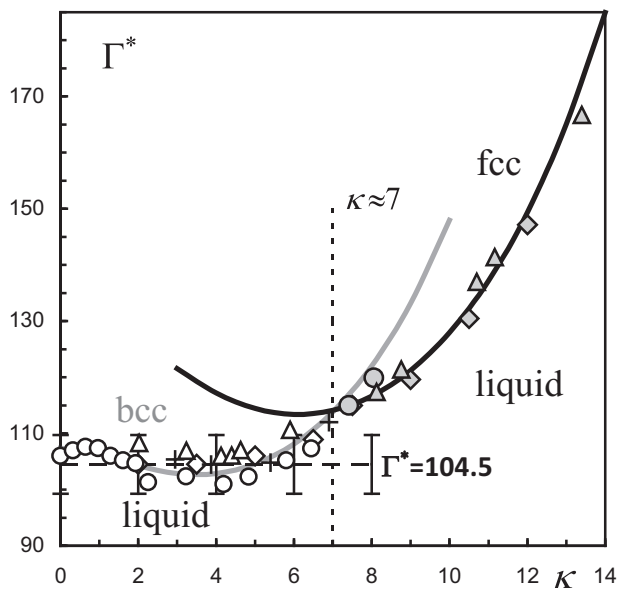

FIG. 1. Melting curves $\Gamma^*(\kappa)$ for 3D Yukawa systems. The symbols correspond to the numerical simulation results (white, for bcc lattice; gray, for fcc): (◇;◆) the results presented in this paper for dissipative structures; and the results for frictionless systems: (+) Ref. [10]; (○;●) Refs. [8,9]; (△;▲) Ref. [11]. Solid lines denote the analytical curves (12): gray for bcc lattice, and black for fcc. The bars correspond to the deviation of $\pm 5\%$ from $\Gamma^* = 104.5$, see Eq. (2).

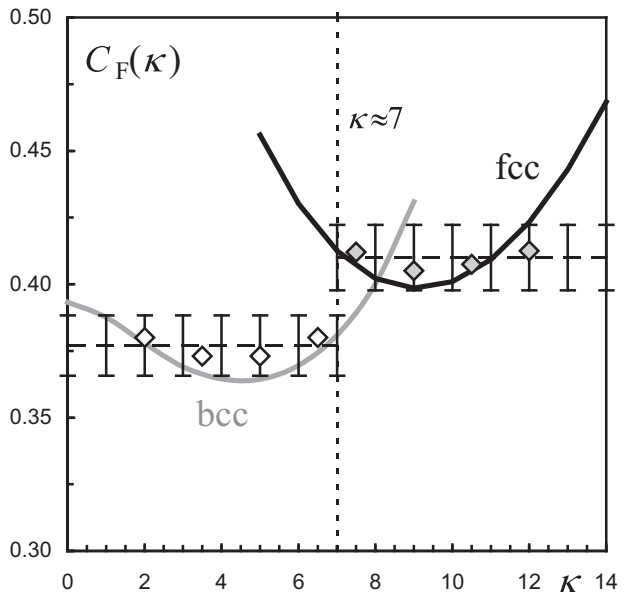

FIG. 3. The coefficient $C_F = \langle \delta F^2 \rangle / (r_p^2 M^2 \omega^{*4})$ vs κ on the melting lines of 3D Yukawa systems. The symbols (◇;◆) denote the results of numerical simulation (white symbols correspond to bcc lattice, gray symbols to fcc).The bars correspond to the deviation of 3% from the average fluctuation level (the dashed horizontal lines). The solid lines correspond to the analytical curves (13), gray to the bcc lattice, and black to the fcc.

in the case of 3D systems, the difference between the position of the melting curve for the fcc lattice and the criterion given by (2) grows with increasing κ. In the case of 2D structures, the melting points for our simulations, as well as the data of Refs. [31–35], correspond to Eq. (4): $\Gamma^*(\kappa) \cong 102.5 \pm 4$ for both frictionless and dissipative systems (see Fig. 2). The bars of the dashed line correspond to the deviation of $\pm 5\%$ from $\Gamma^* = 102.5$ (the dashed line) [see Eq. (4)].

III. THE ANALYSIS OF NUMERICAL RESULTS AND THE APPROXIMATION OF THE MELTING CURVE

To analyze the obtained results, we consider the internal energy density U of the system of particles:

$$U = \frac{m}{2}T + (m-1)\pi n \int_0^\infty \phi(r) g(r) r^{m-1} dr, \qquad (5)$$

where $m = 2, 3$ is the number of dimensions in the system, $g(r)$ is the pair correlation function, and $n = r_p^{-m}$. As the criterion of the change of the type of the lattice we use the minimum of the potential part of the energy U, i.e., the second term in (3). Consider the thermal component $U_T = U - U_0 - 3T/2$ of the potential part of U; here U_0 is the energy density for the crystal lattice at $T = 0$. For any lattice of known type, for example, for the fcc, bcc, or hp lattices, the values of U_0 may be easily computed [23]. Note that in the case of high Γ^* and low κ, the finite cutoff distance r_{cut} has larger influence on the calculations of energy density U; thus the chosen value of r_{cut} should provide convergence of the integral in Eq. (5).

As a matter of convenience we introduce the designation $\Delta r = \delta r / r_{mp}$, where $\delta r = (r - r_{mp})$, and r_{mp} corresponds to the most probable position of the particle in the lattice of a certain type, i.e., the lattice constant: $r_{mp} \equiv r_{bcc} = (3\sqrt{3}/4)^{1/3} r_p$ for the bcc lattice, $r_{mp} \equiv r_{fcc} = 2^{1/6} r_p$ for the fcc lattice, and $r_{mp} \equiv r_{fcc} = (2/\sqrt{3})^{1/2} r_p$ for the hp lattice. So, on the melting line the values of $\sqrt{\langle \Delta r^2 \rangle}$ are equal to $\langle \Delta r^2 \rangle_{bcc}^{1/2} \cong 0.124$ (for bcc lattice), $\langle \Delta r^2 \rangle_{fcc}^{1/2} \cong 0.115$ (for fcc lattice), and $\langle r^2 \rangle_{hp}^{1/2} \cong 0.099\,7$ (for the hp lattice).

Taking into account that the small stochastic declinations Δr from the equilibrium positions of particles are random and described by the normal (Gaussian) distribution law, we see that all the odd moments $\langle \Delta r^{2i+1} \rangle \equiv 0$, and the even moments $\langle \Delta r^{2i} \rangle = \langle \Delta r^2 \rangle^i \prod_{j=1}^{i} (2j-1)$, where i is a non-negative integer. Then, using Taylor series expansion of $\phi(r)$, we get for U_T in the nearest-neighbor approximation,

$$U_T = \frac{N_{nb}}{2} \sum_{i=1}^{\infty} \frac{r_{mp}^{2i}}{(2i)!} \phi_{pm}^{(2i)} \langle \Delta r^{2i} \rangle, \qquad (6)$$

where N_{nb} is the number of the nearest neighbors ($N_{nb} = 8$ for the bcc lattice; $N_{nb} = 12$ for the fcc lattice; $N_{nb} = 6$ for the hp lattice), $\phi_{pm}^{(j)}$ are the jth derivatives of a pair potential $\phi(r)$ at the point of $r = r_{mp}$, and Δr depends on the lattice type and the temperature of particles. The ratio $\delta U = U_T(T\Gamma^*)$ for the bcc and fcc crystal lattices is shown in Fig. 4 for the values of $\langle \Delta r^2 \rangle$ on the melting lines obtained in the numerical simulation ($\langle \Delta r^2 \rangle_{bcc}^{1/2} \cong 0.124$; $\langle \Delta r^2 \rangle_{fcc}^{1/2} \cong 0.115$). One can easily see that the position of the triple point (the point of transition bcc – fcc – liquid) corresponds to $\kappa \cong 7$, thus agreeing well with the results of the numerical simulation shown in Figs. 1(a) and 1(b). Then the nearest-neighbor approximation taking into account the anharmonicity of U_T allows us to obtain adequate physical results.

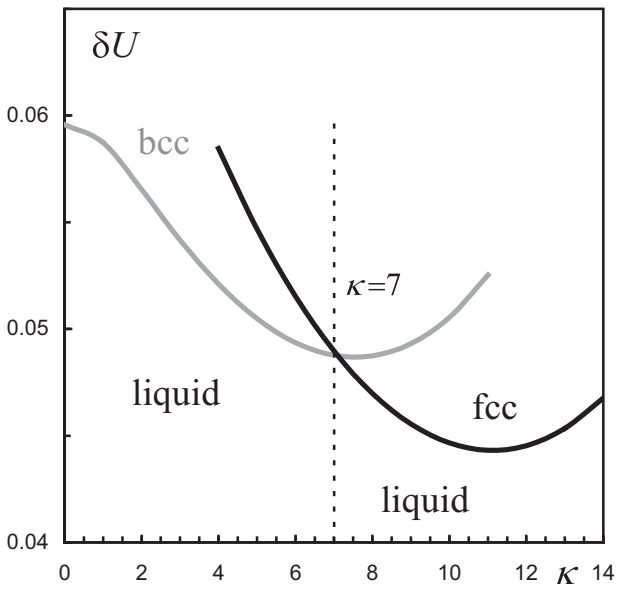

FIG. 4. The functions $\delta U(\kappa)$, gray lines for the bcc lattice, and black for the fcc lattice. $\delta U = U_T/(T\Gamma^*)$, $U_T = U - U_0 - 3T/2$.

Once again we stress that the simple harmonic or quasiharmonic approximations, as well as the fitting of the numerical results by various parametrical functions, do not give reliable information on the position of the phase transition curves (including melting curves) when the form of the parameters of the interparticle interaction potential changes.

The analytical approximation for the phase transition curves of crystal lattices can be found based on the analysis of the equations of motion:

$$M\frac{d\mathbf{V}}{dt} = -M\nu_{fr}\mathbf{V} + eZ\delta\mathbf{E} + F_{ran}, \qquad (7)$$

$$\frac{\partial \delta\mathbf{E}}{\partial t} = -4\pi eZ\delta n\mathbf{V}, \qquad (8)$$

where $\mathbf{V}$ is the thermal velocity of a separate particle, and the influence of the thermal fluctuations of the concentration δn of surrounding particles on its equilibrium position can be considered with the help of the Poisson equation:

$$\mathrm{div}\delta\mathbf{E} = 4\pi eZ\delta n. \qquad (9)$$

Within the framework of the nearest-neighbor approximation, the value of $C_n = 4\pi(eZ)^2\delta n$ can be found with the help of the Taylor series expansion,

$$C_n = N_{nb} \sum_{i=1}^{\infty} \frac{{r_{mp}}^{2i-2} \phi_{pm}^{(2i)}}{(2i-2)!} \langle \Delta r^{2i-2} \rangle, \qquad (10)$$

taking into account that $\langle \Delta r^{2i+1} \rangle \equiv 0$ and the fact that the contributions from the odd derivatives $\phi(r)$ are annihilated in the point of equilibrium.

Hence we can derive two relationships: $\langle eZ\,\delta E\,\delta r\rangle = mT$ and/or $\langle eZ\delta E\rangle^2/(4\pi\delta n) = mT$, which can be used for the definition of the melting criterion of the system. Nevertheless, the analytical evaluation of $\langle eZ\,\delta E\,\delta r\rangle$ and/or $\langle (eZ\delta E)^2\rangle$ for nonlinear systems is complicated enough even within the frames of a nearest-neighbor approximation, because the spatial configuration of a system and the mutual displacements of particles should be thoroughly considered.

For the determination of the positions of melting curves we will use the relation $\langle (eZ\delta E)^2\rangle/(4\pi\delta n) = mT$, where $\delta n = C_n/4\pi(eZ)^2$ (8), and $\langle (eZ\delta E)^2\rangle \cong C_{\rm F} r_{\rm p}^2 M^2\omega^{*4}$ for the values of $\langle\Delta r^2\rangle$ and C_F close to the melting lines of bcc and fcc lattices found in the numerical simulation of the problem; here $m = 2,3$ is the number of dimensions. Hence, after some arithmetical transformations, we obtain

$$\frac{{r_{\rm p}}^2}{TC_n}\left(\frac{\phi^{(2)}}{2}\right)^2 \cong C = \text{const}, \tag{11}$$

and for the coupling parameter on the melting line

$$\Gamma_M^* \cong CC_n\left(\frac{\phi^{(2)}}{2}\right)^{-1}, \tag{12}$$

where $C \cong 7.9 \pm 3\%$ for bcc, $C \cong 11 \pm 3\%$ for fcc, and $C \cong 10.5 \pm 3\%$ for hp lattices; $\{\phi^{(2)}/2\}^{1/2} \equiv \{(eZ)^2(1+\kappa+\kappa^2/2)\exp(-\kappa)/(r_p^3)\}^{1/2}$. The analytical curves (12) are shown in Figs. 1 and 2. A good agreement between the analytical curves and our numerical data can be stated for both 2D and 3D Yukawa systems; the difference between them doesn't exceed 3%. The numerical data of various works [8–11,31–35] are also in a good accordance with the relation (12) for both frictionless and dissipative systems within the numerical errors (from ~2% to ~5%), which are discussed in the above-mentioned works. Once again we note that in the case of 2D structures, the melting points for all simulations (including data of Refs. [31–35]) are close to Eq. (4), $\Gamma^*(\kappa) \cong 102.5 \pm 4$ (i.e., $102.5 \pm 4\%$), for both frictionless and dissipative systems (see Fig. 2), that (in turn) well enough corresponds to theoretical results, as the analytical curve (12) for 2D structures deviates from a constant value $\Gamma^*(\kappa) = 102.5$ in limits $\pm 5\%$ for all κ from 0 to 9.

In the conclusion of this paragraph we consider the possibility of using a formal approach for analytical evaluations of $\langle\delta E\delta r\rangle$ and $\langle (eZ\delta E)^2\rangle$ in the case of 3D systems. The choice of 3D systems is defined by the fact that bcc and fcc lattices have simple 3D (cubic) symmetry, unlike 2D hp lattices with geometry more difficult for the analytical calculations. The basis for this (formal) approach is the following relationships for correlators of studied systems: $\delta\boldsymbol{E} = \delta\boldsymbol{E}_0 + \delta\boldsymbol{E}_{nb}$; $\langle\delta E_0\delta E_{nb}\rangle = 0$; $\langle\delta E^2\rangle = \langle\delta E_0^2\rangle + \langle\delta E_{nb}^2\rangle$; $\delta\boldsymbol{r} = \delta\boldsymbol{r}_0 + \delta\boldsymbol{r}_{nb}$; $\langle\delta r_0\delta r_{nb}\rangle = 0$; $\langle\delta r^2\rangle = \langle\delta r_0^2\rangle + \langle\delta r_{nb}^2\rangle$; $\langle\delta E\delta r\rangle = \langle\delta E_{nb}\delta r_{nb}\rangle + \langle\delta E_0\delta r_0\rangle$.Here δr_0 and δE_0 stand for the displacement of a single (central) particle from its equilibrium position and for the electric field acting on this particle in the assumption of motionless neighbors, respectively; δr_{nb} and δE_{nb} denote the displacements of surrounding particles (the nearest neighbors) from their equilibrium positions and the fluctuations of a field caused by these displacements in a point of equilibrium of a separate (central) particle.

Thus for the $\langle (eZ\delta E)^2\rangle$ value we obtain

$$\langle (eZ\delta E)^2\rangle = \langle (eZ\delta E_0)^2\rangle + \langle (eZ\delta E_{nb})^2\rangle, \tag{13}$$

where

$$\langle (eZ\delta E_{nb})^2\rangle = \frac{3}{8\pi}N_{nb}^2\left\langle\left(\sum_{i=1}^{\infty}\frac{r_{mp}^i}{i!}\,\phi_{pm}^{(i+1)}\Delta r^i\right)^2\right\rangle, \tag{13a}$$

$$\langle (eZ\delta E_0)^2\rangle = \frac{3}{8\pi}\frac{N_{nb}^2}{9}\left\langle\left[\sum_{i=1}^{\infty}\left(\frac{r_{mp}^i}{i!}\,\phi_{pm}^{(i+1)} - \frac{2r_{mp}^{i-1}}{(i-1)!}\,\phi_{pm}^{i}\right)\Delta r^i\right]^2\right\rangle. \tag{13b}$$

Here the normalizing factor $3/8\pi$ is determined by the dimension of system ($m = 3$) and by the probability of a displacement of particle in the chosen direction ($1/4\pi$) on each of the particles considered in pairs (1/2) [15,48,53]; and the averaging of displacements of particles, Δr, follows the relations $\langle\Delta r^{2i}\rangle_{3d} = \frac{\langle\Delta r^2\rangle^i}{3^i}\prod_{j=1}^{i}(2j+1)$; $\langle\Delta r^{2i+1}\rangle_{3d} \equiv 0$. (The difference between $\langle\Delta r^{2i}\rangle_{3d}$ and $\langle\Delta r^{2i}\rangle$ is defined by the necessity of taking into account the dimension of a system (i.e., the directions of displacements of separate particles), unlike the case of averaging for scalar characteristics (U,δn) which are described by function $g(r)$ with radial symmetry. Comparison of Eq. (13) with the results of numerical experiments shows their good accordance for the screening parameters $\kappa \leqslant 12$, used for the simulation (see Fig. 3).

Within the limits of the considered approach, we can write for the value of $\langle eZ\,\delta E\,\delta r\rangle$,

$$\langle eZ\delta E\delta r\rangle = \langle eZ\delta E_{nb}\delta r_{nb}\rangle + \langle eZ\delta E_0\delta r_0\rangle, \tag{14}$$

where

$$\langle eZ\,\delta E_{nb}\delta r_{nb}\rangle = \frac{3}{8\pi}N_{nb}\sum_{i=1}^{\infty}\frac{r_{mp}^{2i}}{(2i-1)!}\,\phi_{pm}^{(2i)}\langle\Delta r^{2i}\rangle_{3d}, \tag{14a}$$

$$\langle eZ\delta E_0\delta r_0\rangle = \frac{3}{8\pi}\frac{N_{nb}}{3}\sum_{i=1}^{\infty}\left(\frac{r_{mp}^{2i}}{(2i-1)!}\,\phi_{pm}^{(2i)} - \frac{2r_{mp}^{2i-1}}{(2i-2)!}\,\phi_{pm}^{(2i-1)}\right)\langle\Delta r^{2i}\rangle_{3d}. \tag{14b}$$

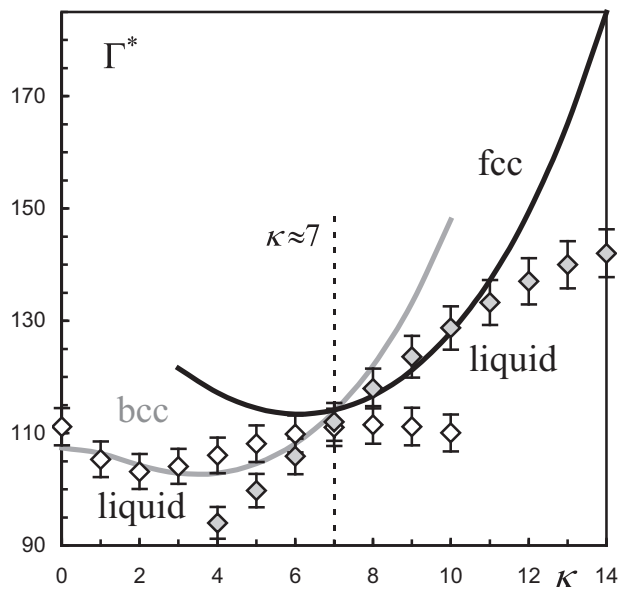

FIG. 5. Melting curves $\Gamma^*(\kappa)$ for 3D Yukawa systems. Solid lines denote the analytical curves (10), gray for the bcc lattice, and black for the fcc. The symbols correspond to the approximation (15), white for the bcc lattice, and black for the fcc.

As a result, using $\langle eZ\,\delta E\,\delta r\rangle = 3T$, we will receive the following value of Γ^* on the melting line for the bcc and fcc lattices:

$$\Gamma^*_M \cong \Gamma \frac{3}{\langle eZ\,\delta E\,\delta r\rangle}\left(\frac{\phi^{(2)}}{2}\right). \tag{15}$$

Comparison of approximations (12) and (15) is shown in Fig. 5. It is easy to see that the distinction between them grows with the growth of the screening parameter (at $\kappa > 11$). It may result from the use of simplified correlators of a system which does not allow one to fully take into account the influence of mutual displacements of particles. Nevertheless, Eq. (12) gives good accordance with the results of numerical experiments for 3D systems up to $\kappa \sim 13$–14, and also for 2D systems for $\kappa \leqslant 8$.

Finally, we note again that the consideration of the anharmonicity of the potential gives a good result, even in the nearest-neighbor approximation. The influence of nonlinearity (anharmonicity) of pair interaction forces on the position of melting curves was considered earlier in several works [9,18,19] only for polymorphous fcc-bcc transformations. We should also note the attempt to take into account the nonlinearity of forces that was made in [48], but this approximation was based on fitting of the numerical data.

IV. CONCLUSION

In this work, the melting of fcc, bcc, 3D lattices, and the hp 2D lattice was studied analytically and numerically for the systems with the Yukawa pair interactions. The Lindemann parameter, the coupling parameter, and the density of the thermal fluctuations of pair forces have been obtained near the melting lines of Yukawa systems for a wide range of their parameters. Our simulations have shown that the dissipation (i.e., the friction) practically does not affect the above-listed parameters of Yukawa systems near the solid-liquid phase transitions, including the position of the melting curves. Comparison of the obtained results with the existing theoretical and numerical data is presented for both frictionless and dissipative systems.

Characteristic frequencies and internal energy densities in crystal lattices were estimated within the framework of the nearest-neighbor approximation, and the amplitudes of the oscillations of particles in the nodes of the lattice were evaluated with the help of the Lindemann parameter on the melting lines of the systems under study.

Analytical approaches, taking into account the influence of nonlinearity (anharmonicity) of the pair interaction forces, for the determination of equilibrium melting curves and thermal fluctuations of the electric field are proposed (see Sec. III). It is necessary to emphasize that both the numerical and theoretical data on the density of the thermal fluctuations for pair forces in the Yukawa systems have been received.

On the basis of the developed theoretical model, an analytical approximation for the melting phase curves also was obtained for solid-liquid transitions in the fcc, bcc, and hp lattices for the Yukawa systems. Unlike existing approximations [7–22,42–46], the proposed approach does not lean upon the empirical fitting of numerical data by arbitrary polynomial functions and/or on the semiempirical models (which are based on the simple harmonic or quasiharmonic approximations) and can be used for analysis of the melting conditions with the changes of interparticle interactions in a wide range of screening parameters.

The additional advantages of the proposed model (distinguishing it from earlier existing theories) is that all parities are presented in the general form (including derivatives of potential of pair interactions) and can be used for a more general class of interparticle interactions. Thus we have to note that the scope of the proposed approach is not limited by the considered Yukawa systems. The presented model may be easily adapted for a wide range of systems with various isotropic potentials and may be useful for determinations of solid-liquid phase curves in 2D and 3D systems and for estimations of fcc-bcc-liquid triple points in 3D, too.

ACKNOWLEDGMENTS

This work was supported by the Russian Foundation for Basic Research (Grants No. 13-08-00263, No. 14-08-31633, No. 14-02-31226) the Ministry of Education and Science of the Russian Federation and by the Program of the Presidium of the Russian Academy of Sciences.

[1] *Intermolecular Interactions: From Diatomics to Biopolymers*, edited by B. Pullman (Wiley Interscience, Chichester, UK, 1978).

[2] A. A. Ovchinnikov, S. F. Timashev, and A. A. Belyy, *Kinetics of Diffusion Controlled Chemical Processes* (Nova Science Publishers, Commack, NY, 1989).

[3] N. H. March and M. P. Tosi, *Introduction to Liquid State Physics* (World Scientific, Singapore, 1995).

[4] S. V. Vladimirov, K. Ostrikov, and A. A. Samarian, *Physics and Applications of Complex Plasmas* (Imperial College, London, 2005).

[5] *Complex and Dusty Plasmas*, edited by V. E. Fortov and G. E. Morfill (CRC Press, Boca Raton, FL, 2010).

[6] A. Ivlev, G. Morfill, H. Lowen, and C. P. Royall, *Complex Plasmas and Colloidal Dispersions: Particle-Resolved Studies of Classical Liquids and Solids* (World Scientific, Singapore, 2012).

[7] B. A. Klumov, Physics - Uspekhi **53**, 1053 (2010).

[8] R. T. Farouki and S. Hamaguchi, J. Chem. Phys. **101**, 9885 (1994).

[9] S. Hamaguchi, R. T. Farouki, and D. H. E. Dubin, Phys. Rev. E **56**, 4671 (1997).

[10] E. J. Meijer and D. Frenkel, J. Chem. Phys. **94**, 2269 (1991).

[11] M. J. Stevens and M. O. Robbins, J. Chem. Phys. **98**, 2319 (1993).

[12] R. S. Hoy and M. O. Robbins, Phys. Rev. E **69**, 056103 (2004).

[13] M. O. Robbins, K. Kremer, and G. S. Grest, J. Chem. Phys. **88**, 3286 (1988).

[14] O. S. Vaulina and S. A. Khrapak, JETP **90**, 287 (2000).

[15] O. S. Vaulina, S. V. Vladimirov, O. F. Petrov, and V. E. Fortov, Phys. Rev. Lett. **88**, 245002 (2002).

[16] O. S. Vaulina, S. V. Vladimirov, O. F. Petrov, and V. E. Fortov, Phys. Plasmas **11**, 3234 (2004).

[17] D. H. E. Dubin and H. Dewitt, Phys. Rev. B **49**, 3043 (1994).

[18] W. G. Hoover, D. A. Young, and R. Grover, J. Chem. Phys. **56**, 2207 (1972).

[19] W. G. Hoover, S. G. Gray, and K. W. Johnson, J. Chem. Phys. **55**, 1128 (1971).

[20] S. A. Khrapak and G. E. Morfill, Europhys. Lett. **100**, 66004 (2012).

[21] V. Heinonen, A. Mijailović, C. V. Achim, T. Ala-Nissila, R. E. Rozas, J. Horbach, and H. Löwen, J. Chem. Phys. **138**, 044705 (2013).

[22] O. S. Vaulina, S. A. Khrapak, and G. E. Morfill, Phys. Rev. E **66**, 016404 (2002).

[23] O. S. Vaulina, X. G. Koss, Yu. V. Khrustalyov, O. F. Petrov, and V. E. Fortov, Phys. Rev. E **82**, 056411 (2010).

[24] O. S. Vaulina and I. E. Drangevski, Phys. Scripta **73**, 577 (2006).

[25] O. S. Vaulina and X. G. Koss (Adamovich), Phys. Lett. A **373**, 3330 (2009).

[26] O. S. Vaulina, O. F. Petrov, A. V. Gavrikov, X. G. Adamovich, and V. E. Fortov, Phys. Lett. A **372**, 1096 (2008).

[27] O. S. Vaulina and X. G. Koss, Phys. Lett. A **378**, 3475 (2014).

[28] O. S. Vaulina and E. V. Vasilieva, Europhys. Lett. **106**, 65001 (2014).

[29] O. S. Vaulina and E. V. Vasilieva, Phys. Lett. A **378**, 719 (2014).

[30] O. F. Petrov, M. M. Vasiliev, Ye Tun, K. B. Statsenko, O. S. Vaulina, E. V. Vasilieva, and V. E. Fortov, JETP **120**, 327 (2015).

[31] Qi Wei-Kai, Wang Ziren, Han Yilong, and Chen Yong, J. Chem. Phys. **133**, 234508 (2010).

[32] H. Lowen, J. Phys.: Condens. Matter **4**, 10105 (1992).

[33] X. H. Zheng and J. C. Earnshaw, *Advances in Dusty Plasma*, edited by P. K. Shukla, D. A. Mendis, and T. Desai (World Scientific, Singapore, 1997), p. 188.

[34] X. H. Zheng and J. C. Earnshaw, Europhys. Lett. **41**(6), 635 (1998).

[35] B. K. Clark, M. Casula, and D. M. Ceperley, Phys. Rev. Lett. **103**, 055701 (2009).

[36] I. V. Schweigert, V. A. Schweigert, and F. M. Peeters, Phys. Rev. Lett. **82**, 5293 (1999).

[37] S. Muto and H. Aoki, Phys. Rev. B **59**, 14911 (1999).

[38] P. Hartmann, G. J. Kalman, and Z. Donko, J. Phys. A: Math. Gen. **39**, 4485 (2006).

[39] M. Mazars, arXiv:1301.1571.

[40] A. Derzsi, A. Zs. Kovacs, Z. Donko, and P. Hartmann, Phys. Plasmas **21**, 023706 (2014).

[41] K. Zahn and G. Maret, Phys. Rev. Lett. **85**, 3656 (2000).

[42] B. A. Klumov, Y. Jin, and H. A. Makse, J. Phys. Chem. B **118**, 10761 (2014).

[43] T. Zykova-Timan, J. Horbach, and K. Binder, J. Chem. Phys. **133**, 014705 (2010).

[44] R. E. Rozas and J. Horbach, Europhys. Lett. **93**, 26006 (2011).

[45] A. Härtel, M. Oettel, R. E. Rozas, S. U. Egelhaaf, J. Horbach, and H. Löwen, Phys. Rev. Lett. **108**, 226101 (2012).

[46] S. A. Khrapak, M. Chaudhuri, and G. E. Morfill, J. Chem. Phys. **134**, 241101 (2011).

[47] O. S. Vaulina, E. A. Lisin, A. V. Gavrikov, O. F. Petrov, and V. E. Fortov, Phys. Rev. Lett. **103**, 035003 (2009).

[48] O. S. Vaulina and E. V. Vasilieva, Europhys. Lett. **95**, 55004 (2011).

[49] S. A. Khrapak, M. Chaudhuri, and G. E. Morfill, Phys. Rev. B **82**, 052101 (2010).

[50] D. R. Nelson and B. I. Halperin, Phys. Rev. B **19**, 2457 (1979).

[51] J. M. Kosterlitz and D. J. Thouless, J. Phys. C **6**, 1181 (1973).

[52] A. P. Young, Phys. Rev. B **19**, 1855 (1979).

[53] E. M. Lifshitz and L. P. Pitaevskii, *Physical Kinetics* (Pergamon Press, Oxford, 1981).